ARTICLE

A Novel Bidirectional Interaction Model and Electric Energy Measuring Scheme of EVs for V2G with Distorted Power Loads

Jiarui Cui[1,2,*], Qing Li[1,*], Bin Cao[2,3], Xiangquan Li[1] and Qun Yan[1]

[1]School of Automation and Electrical Engineering, University of Science and Technology Beijing, Beijing, 100083, China

[2]Guiyang Aluminum Magnesium Design and Research Institute Co., Ltd., Guiyang, 550081, China

[3]Chinalco Intelligent Technology Development Co., Ltd., Hangzhou, 311199, China

*Corresponding Authors: Jiarui Cui. Email: cuijiarui@ustb.edu.cn; Qing Li. Email: liqing@ies.ustb.edu.cn

ABSTRACT

With the increasing demand for petroleum resources and environmental issues, new energy electric vehicles are increasingly being used. However, the large number of electric vehicles connected to the grid has brought new challenges to the operation of the grid. Firstly, A novel bidirectional interaction model is established based on modulation theory with nonlinear loads. Then, the electric energy measuring scheme of EVs for V2G is derived under the conditions of distorted power loads. The scheme is composed of fundamental electric energy, fundamental-distorted electric energy, distorted-fundamental electric energy and distorted electric energy. And the characteristics of each electric energy are analyzed. Finally, the correctness of the model and energy measurement method is verified by three simulation cases: the impact signals, the fluctuating signals, and the harmonic signals.

KEYWORDS

Electric vehicles; V2G; energy metering; bidirectional interaction model; electric energy measuring scheme

1 Introduction

Electric vehicles (EVs) play a critical role in meeting the environmental goals of the Sustainable Development Scenario to reduce local air pollution and to address climate change [1]. With the increasing demand for petroleum resources and environmental issues, new energy electric vehicles are increasingly being put into use in the last decade. The number of electric cars on the world's roads had swelled to 7.2 million by 2019 from only about 17000 in 2010 [2]. EVs could actively provide about 460 GWh of energy to the grid at suitable times via vehicle-to-grid services (V2G). But every coin has two sides, and there are a lot of challenges to unlock the full flexibility potential of electric vehicles, such as technologies, regulatory, market frameworks, and so on.

V2G technology has been widely concerned by experts and scholars all over the world, and has achieved a series of results which mainly focus on scheduled charging and discharging [3–6], bidirectional converter [7–9], power energy management system [10,11], battery lifecycle [12], modeling approaches [13], energy storage systems [14] and so on. It is pointed out in [15] that

a large amount of energy storage needs to consider the fast-dynamic response of power demand and a modular method is given. A green V2G network is proposed in [16] for energy management which consists of three planes: management plane, control plane, and data plane. Literature [17,18] mainly studies aspects of data security and communication security. V2G technology enables electric vehicles to deliver power to the power system to provide complementary capabilities. Literature [17] established a novel and secure communication framework to meet the real-time and security of power transportation. Literature [18] proposed a member-based secure data sharing scheme in V2G networks to protect data privacy and save system resources. In [19], a battery state based scheduling algorithm is proposed to optimize the V2G charging and discharging strategy. In [20], a construction scheme based on transfer learning is proposed to update the safe charging and discharging strategy dynamically. These documents have played a pivotal role in the development of V2G technology. In [21], based on grid load time-sharing pricing, an electric vehicle scheduling model was established with the goal of reducing charging cost and network loss cost. The charging and discharging strategies of electric vehicles were obtained by real-time calculation of power flow calculation and convex optimization algorithm. Literature [22] proposes a V2G management system consisting of an ordered charging dispatch system and a V2G converter control system. The system can fully utilize the flexibility of electric vehicle load while meeting the charging needs of electric vehicles. In [23], an ordered charge and discharge control model in V2G mode is proposed, in order to reduce the charge and discharge cost of electric vehicles and the variance of grid load.

However, electric energy measuring methods for V2G have not been concerned widely, although there have been a large number of mature modeling methods [24–26], filtering algorithms [27–29], measurement techniques [30–32] and they have been successfully applied to actual systems in the field of industrial processes. Based on the idea of [33], we established the charging model and discharging model of EVs for V2G, and given the electric energy measuring formula in [34]. But they did not consider the effect of the distorted power loads that is always stayed in power grid when EVs are charging or discharging. Furthermore, the unified bidirectional model and the corresponded electric energy measuring methods did not discuss. With the widespread use of V2G technology, it will be a very effective means to increase the participation of EV owners in V2G. So, this paper proposes a bidirectional electric energy measuring scheme for V2G with distorted power loads which considered the great randomness of the charging and discharging time of EVs and the distorted power loads on the power grid.

The rest of this paper is presented as follows. Section 2 establishes the bidirectional interaction model of EVs for V2G based on electric network theory. In Section 3, a bidirectional electric energy measuring scheme is proposed for V2G with distorted power loads based on power flow analysis and energy metering theory. Section 4 gives the simulation results and analyzes the data. Finally, the conclusions are shown in Section 5.

2 A Bidirectional Interaction Model of EVs for V2G

The signals' type is very complex because of the large number of non-linear loads in the grid. In addition to harmonic signals and inter-harmonic signals, there are many other forms of distorted signals such as impact signals and fluctuation signals which are typical in grid. They cannot be described by harmonic models. We can establish their model as follows using modulation theory:

$$i_k(t) = (1 + \alpha_k(t))I_m \sin(\omega_0 t + \phi_k) \tag{1}$$

where k is the k-th impact or fluctuation, $\alpha_k(t)$ is a random function, ϕ_k are random variables, I_m is the amplitude of current. In order to facilitate the measurement, the zero point of the measurement time is based on the time at which $\alpha_k(t)$ occurs.

If the signal is an impact signal, $\alpha_k(t)$ can be approximated as follows:

$$\alpha_k(t) = M_k e^{-\frac{t}{\tau_k}}, (M_k > 0) \tag{2}$$

If the signal is a fluctuating signal, $\alpha_k(t)$ can be approximated as follows:

$$\alpha_k(t) = \begin{cases} M_k, & 0 < t < \tau_k, \\ 0, & \text{other} \end{cases}, \quad (M_k > 0) \tag{3}$$

where the duration τ_k is random since occur time of the impact or fluctuation signals is uncertain. M_k is the amplitude of the impact or fluctuating signal.

Under the condition of distortion signal, the voltage at a certain measuring point in the power grid and the current flowing into the measuring point can be expressed as follows:

$$u(t) = u_I(t) + u_S(t) \tag{4}$$

$$i(t) = i_I(t) + i_S(t) \tag{5}$$

where $u_I(t)$ and $i_I(t)$ are the fundamental voltage at metering point and the current flowing into the metering point, respectively, $u_S(t)$ and $i_S(t)$ are the distortion voltage and the current, respectively.

On the basis of [33] and [34], a bidirectional interaction model of EVs for V2G is established as shown in Fig. 1.
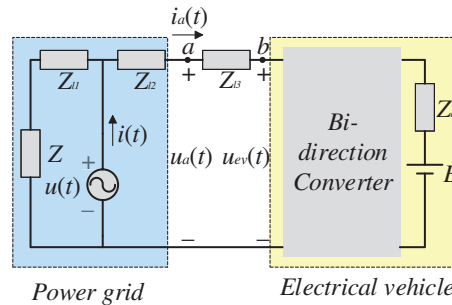

Figure 1: Bidirectional interaction model of electric vehicles in the power grid

In Fig. 1, the left side of the circuit is a simplified model of the grid, where $u(t)$ is the grid voltage and $i(t)$ is the grid current. Z_{l1}, Z_{l2}, Z_{l3} are line loads in the grid. Z is the other load in the grid. The right side of the circuit is an electric car, where E is the electric vehicle battery electromotive force, Z_{ev} is the internal load of electric vehicle. $u_a(t)$ is the voltage at the metering point a, and $i_a(t)$ is the current flowing into the metering point a. $u_{ev}(t)$ is the output voltage when the electric vehicle is discharged to the grid. If there are no other loads Z, then the model is simplified to the model in [34].

3 A Bidirectional Electric Energy Measuring Scheme

Assuming that the grid voltage is assumed to be as follows:

$$u(t) = U_m \sin(\omega_0 t + \psi_k) \tag{6}$$

where voltage phase ψ_k is a random variable and U_m is the amplitude of voltage.

Assuming the current direction shown in Fig. 1 is the positive direction, that is, the charging direction of the electric vehicle is the positive direction. According to formula (1), the current at the metering point a when charging the electric vehicle is as follows:

$$i_a(t) = (1 + \alpha(t)) I_m \sin(\omega_0 t + \phi_k) \tag{7}$$

When the electric vehicle is discharged, the current at the measuring point a is as follows:

$$i_a(t) = -(1 + \alpha(t)) I_m \sin(\omega_0 t + \phi_k) \tag{8}$$

When the electric vehicle is charged in the power grid, the voltage at the measuring point a is as follows:

$$u_a(t) = u(t) - Z_{l2} i_a(t) \tag{9}$$

When the electric vehicle is discharged into the power grid, the voltage at the measuring point a is as follows:

$$u_a(t) = u_{ev}(t) + Z_{l3} i_a(t) \tag{10}$$

In fact, the output voltage $u_{ev}(t)$ is the same as the grid voltage when the EVs are discharged, and is a standard sinusoidal voltage.

$$u_{ev}(t) = u(t) \tag{11}$$

Assuming that Z_{l2} and Z_{l3} are pure resistive loads R_l. In the case of V2G charging or discharging, the voltage at the measuring point a can be expressed as follows:

$$u_a(t) = u(t) - R_l \cdot (1 + \alpha_k(t)) I_{mk} \sin(\omega_0 t + \phi_k) \tag{12}$$

Take the k-th impact and fluctuation signal as an example for analysis. For the k-th impact or fluctuation, the voltage at the measuring point a is as follows:

$$
\begin{aligned}
u_{ak}(t) &= U_m \sin(\omega_0 t + \psi_k) - R_l (1 + \alpha_k(t)) I_m \sin(\omega_0 t + \varphi_k) \\
&= U_m \sin(\omega_0 t + \psi_k) - R_l I_m \sin(\omega_0 t + \varphi_k) - R_l \alpha_k(t) I_m \sin(\omega_0 t + \varphi_k) \\
&= U_m \sin \omega_0 t \cos \psi_k + U_m \sin \psi_k \cos \omega_0 t - R_l I_m \sin \omega_0 t \cos \varphi_k \\
&\quad - R_l I_m \sin \varphi_k \cos \omega_0 t - R_l I_m \alpha_k(t) \sin(\omega_0 t + \varphi_k) \\
&= u_{akI}(t) + u_{aks}(t)
\end{aligned} \tag{13}
$$

According to formula (13), the voltage at the metering point a can be divided into a fundamental voltage and a distortion voltage. The fundamental voltage at the metering point a is as follows:

$$
\begin{aligned}
u_{akI}(t) &= U_m \sin \omega_0 t \cos \psi_k + U_m \sin \psi_k \cos \omega_0 t - R_l I_m \sin \omega_0 t \cos \varphi_k \\
&\quad - R_l I_m \sin \varphi_k \cos \omega_0 t
\end{aligned}
$$

$$
\begin{aligned}
&= (U_\mathrm{m} \cos \psi_k - R_l I_\mathrm{m} \cos \varphi_k) \sin \omega_0 t \\
&\quad + (U_\mathrm{m} \sin \psi_k - R_l I_\mathrm{m} \sin \varphi_k) \cos \omega_0 t \\
&= U_{akI\mathrm{m}} \sin (\omega_0 t + \theta_k)
\end{aligned} \tag{14}
$$

The fundamental voltage amplitude is as follows:

$$
\begin{aligned}
U_{ak\mathrm{Im}} &= \sqrt{(U_\mathrm{m} \cos \psi_k - R_l I_\mathrm{m} \cos \varphi_k)^2 + (U_\mathrm{m} \sin \psi_k - R_l I_\mathrm{m} \sin \varphi_k)^2} \\
&= \sqrt{U_\mathrm{m}^2 + R_l^2 I_\mathrm{m}^2 - 2 U_\mathrm{m} R_l I_\mathrm{m} \cos (\varphi_k - \psi_k)}
\end{aligned} \tag{15}
$$

The fundamental voltage phase is as follows:

$$
\theta_k = \arctan \frac{U_m \sin \psi_k - R_l I_m \sin \phi_k}{U_m \cos \psi_k - R_l I_m \cos \phi_k} \tag{16}
$$

The distortion voltage at the metering point a is as follows:

$$
u_{akS}(t) = -R_l I_m \alpha_k(t) \sin (\omega_0 t + \phi_k) \tag{17}
$$

According to Eq. (5), the current flowing into the metering point a can be divided into a fundamental current and a distortion current. The fundamental current is as follows:

$$
i_{akI}(t) = -I_m \sin (\omega_0 t + \phi_k) \tag{18}
$$

The distortion current is as follows:

$$
i_{akS}(t) = -I_m \alpha_k(t) \sin (\omega_0 t + \phi_k) \tag{19}
$$

Assume that within the measurement time ($T = N \cdot T_0$, where T_0 is the fundamental period.), the charging time of the electric vehicle is T_1, and the discharging time is T_2. Theoretically, there is $P_1 > P_2$, where P_1 is the total power charged and P_2 is the total power discharged. In order to facilitate the measurement, it is assumed that in the measurement time T, the N_1 times impact occurs in the charging process, and the charging measurement time is $T_1 = N_1 T_0$, the N_2 times impact occurs in the discharging process, and the discharging measurement time is $T_2 = N_2 T_0$. The average power at point a is as follows:

$$
\begin{aligned}
P_a &= \frac{1}{T} \sum_{k=1}^{N_1+N_2} \int_0^{T_1+T_2} p_{ak}(t) dt \\
&= \frac{1}{T} \left(\sum_{k=1}^{N_1} \int_0^{T_1} p_{ak\_\mathrm{G2V}}(t) dt + \sum_{k=1}^{N_2} \int_{T_2}^{T_1+T_2} p_{ak\_\mathrm{V2G}}(t) dt \right) \\
&= \frac{1}{T} \left(P_{a\_\mathrm{G2V}} T_1 + P_{a\_\mathrm{V2G}} T_2 \right)
\end{aligned} \tag{20}
$$

Therefore, the electrical energy at point a is as follows:

$$
W_a = T P_a = P_{a\_\mathrm{G2V}} T_1 + P_{a\_\mathrm{V2G}} T_2
$$

$$= \left(P_{I\_G2V} + P_{IS\_G2V} + P_{SI\_G2V} + P_{S\_G2V} \right) T_1$$

$$+ \left(P_{I\_V2G} + P_{IS\_V2G} + P_{SI\_V2G} + P_{S\_V2G} \right) T_2$$

$$= \left(P_{I\_G2V} T_1 + P_{I\_V2G} T_2 \right) + \left(P_{IS\_G2V} T_1 + P_{IS\_V2G} T_2 \right)$$

$$+ \left(P_{SI\_G2V} T_1 + P_{SI\_G2V} T_2 \right) + \left(P_{S\_G2V} T_1 + P_{S\_V2G} T_2 \right)$$

$$= W_I + W_{IS} + W_{SI} + W_S \tag{21}$$

According to the formula (21), the electrical energy at the point a can be divided into four parts:

$$W_I = W_{I\_G2V} + W_{I\_V2G} = P_{I\_G2V} T_1 + P_{I\_V2G} T_2 \tag{22}$$

$$W_{IS} = W_{IS\_G2V} + W_{IS\_V2G} = P_{IS\_G2V} T_1 + P_{IS\_V2G} T_2 \tag{23}$$

$$W_{SI} = W_{SI\_G2V} + W_{SI\_V2G} = P_{SI\_G2V} T_1 + P_{SI\_V2G} T_2 \tag{24}$$

$$W_S = W_{S\_G2V} + W_{S\_V2G} = P_{S\_G2V} T_1 + P_{S\_V2G} T_2 \tag{25}$$

Taking the discharge situation of electric vehicles as an example, this paper will analyze the four parts of electrical energy in turn.

3.1 Fundamental Power

Combining Eqs. (14) and (18), the fundamental components of the average power of point a is as follows:

$$P_{I\_V2G} = \sum_{k=1}^{N_2} \frac{1}{T_2} \int_{T_1}^{T_1+T_2} u_{akI}(t) i_{akI}(t) dt$$

$$= -\sum_{k=1}^{N_2} \frac{1}{T_2} \int_{T_1}^{T_1+T_2} \{ U_{akIm} \sin(\omega_0 t + \theta_k) \cdot I_m \sin(\omega_0 t + \varphi_k) \} dt$$

$$= \frac{1}{2} \sum_{k=1}^{N_2} \frac{1}{T_2} \int_{T_1}^{T_1+T_2} U_{akIm} I_m \cos(2\omega_0 t + \theta_k + \varphi_k) dt$$

$$- \frac{1}{2} \sum_{k=1}^{N_2} \frac{1}{T_2} \int_{T_1}^{T_1+T_2} U_{akIm} I_m \cos(\theta_k - \varphi_k) dt \tag{26}$$

In Eq. (26), the first part is the second harmonic component of the power, and the integral mean is zero. Additionally, there is $U_{akIm} > 0$, $I_m > 0$ and $\cos(\theta_k - \phi_k)$, so the first part must be positive. In summary, the following conclusion can be drawn:

$$W_{I\_V2G} = T_2 P_{I\_V2G}$$

$$= -\frac{1}{2} \sum_{k=1}^{N_2} \int_{T_1}^{T_1+T_2} U_{kIm\_V2G} I_m \cos(\theta_{k\_V2G} - \varphi_k) dt < 0 \tag{27}$$

3.2 Power Generated by Fundamental Voltage and Distortion Current

Combining Eqs. (14) and (19), the instantaneous power generated by the fundamental voltage and distortion current at point a is as follows:

$$u_{akI}(t)i_{aks}(t) = -U_{ak\text{Im}}\sin(\omega_0 t + \theta_k) \cdot I_m\alpha_k(t)\sin(\omega_0 t + \phi_k) \tag{28}$$

For the impact or fluctuating signals, the cumulative time of energy can be considered to be infinite. Therefore, the electric energy generated by the fundamental voltage and the distorted current at point a is as follows:

$$W_{IS\_V2G} = -\sum_{k=1}^{N_2}\int_0^\infty U_{ak\text{Im}}\sin(\omega_0 t + \theta_k) \cdot I_m\alpha_k(t)\sin(\omega_0 t + \varphi_k)\,dt$$

$$= \frac{1}{2}\sum_{k=1}^{N_2}\int_0^\infty U_{ak\text{Im}} \cdot I_m\alpha_k(t)\left[\cos(2\omega_0 t + \theta_k + \varphi_k) - \cos(\theta_k - \varphi_k)\right]dt$$

$$= \frac{1}{2}\sum_{k=1}^{N_2}\int_0^\infty U_{ak\text{Im}} \cdot I_m\alpha_k(t)\cos(2\omega_0 t + \theta_k + \varphi_k)\,dt$$

$$- \frac{1}{2}\sum_{k=1}^{N_2}\int_0^\infty U_{ak\text{Im}} \cdot I_m\alpha_k(t)\cos(\theta_k - \varphi_k)\,dt \tag{29}$$

The first term in Eq. (29) is denoted by A, and the second term is denoted by B. When $\alpha_k(t)$ is an impact signal, combining Eqs. (2) and (29), A and B can be simplified as follows:

$$A = \frac{1}{2}\sum_{k=1}^{N_2}U_{ak\text{Im}}I_m M_k\int_0^\infty e^{-\frac{1}{\tau_k}}\cos(2\omega_0 t + \theta_k + \varphi_k)\,dt$$

$$= \frac{1}{4}\sum_{k=1}^{N_2}U_{ak\text{Im}}I_m M_k\int_0^\infty e^{-\frac{1}{\tau_k}}(e^{j(2\omega_0 t + \theta_k + \varphi_k)} + e^{-j(2\omega_0 t + \theta_k + \varphi_k)})\,dt$$

$$= \frac{1}{4}\sum_{k=1}^{N_2}U_{ak\text{Im}}I_m M_k\left[e^{j(\theta_k + \varphi_k)}\int_0^\infty e^{\left(2j\omega_0 - \frac{1}{\tau_k}\right)t}\,dt + e^{-j(\theta_k + \varphi_k)}\int_0^\infty e^{-\left(2j\omega_0 + \frac{1}{\tau_k}\right)t}\,dt\right]$$

$$= \frac{1}{4}\sum_{k=1}^{N_2}U_{ak\text{Im}}I_m M_k\left[\frac{e^{-j(\theta_k + \varphi_k)}}{2j\omega_0 + \frac{1}{\tau_k}} - \frac{e^{j(\theta_k + \varphi_k)}}{2j\omega_0 - \frac{1}{\tau_k}}\right]$$

$$= \frac{1}{4}\sum_{k=1}^{N_2}U_{ak\text{Im}}I_m M_k\tau_k\frac{(2j\omega_0\tau_k - 1)e^{-j(\theta_k + \varphi_k)} - (2j\omega_0\tau_k + 1)e^{j(\theta_k + \varphi_k)}}{(2j\omega_0\tau_k + 1)(2j\omega_0\tau_k - 1)}$$

$$= \frac{1}{4}\sum_{k=1}^{N_2}U_{ak\text{Im}}I_m M_k\tau_k\frac{2j\omega_0\tau_k(-2j\sin(\theta_k + \varphi_k)) - 2\cos(\theta_k + \varphi_k)}{-(4\omega_0^2\tau_k^2 + 1)}$$

$$= \frac{1}{2} \sum_{k=1}^{N_2} U_{ak\mathrm{Im}} I_m M_k \tau_k \frac{\cos(\theta_k + \varphi_k) - 2\omega_0 \tau_k \sin(\theta_k + \varphi_k)}{4\omega_0^2 \tau_k^2 + 1}$$

$$= \frac{1}{2} \sum_{k=1}^{N_2} U_{ak\mathrm{Im}} I_m M_k \tau_k \frac{\sin \eta_k}{\sqrt{4\omega_0^2 \tau_k^2 + 1}} \tag{30}$$

$$B = \frac{1}{2} \sum_{k=1}^{N_2} U_{ak\mathrm{Im}} I_m M_k \cos(\theta_k - \varphi_k) \int_0^\infty e^{-\frac{1}{\tau_k}} dt$$

$$= \frac{1}{2} \sum_{k=1}^{N_2} U_{ak\mathrm{Im}} I_m M_k \cos(\theta_k - \varphi_k) \cdot (-\tau_k) \cdot e^{-\frac{1}{\tau_k}} |_0^\infty$$

$$= \frac{1}{2} \sum_{k=1}^{N_2} U_{ak\mathrm{Im}} I_m M_k \tau_k \cos(\theta_k - \varphi_k) \tag{31}$$

In Eq. (30), η_k is as follows:

$$\eta_k = \arctan\left(\frac{1}{2\omega_0 \tau_k}\right) - \phi_k - \theta_k \tag{32}$$

In Eq. (31), all parameters are positive, so there is $B > 0$. A is a small value relative to B. Moreover, A is a random variable whose cumulative of multiple impacts tends to zero. Therefore, the following conclusion can be drawn:

$$W_{IS\_V2G} = A - B < 0 \tag{33}$$

When $\alpha_k(t)$ is a fluctuating signal, combining Eqs. (3) and (29), W_{IS_V2G} can be simplified as follows:

$$W_{IS\_V2G} = \frac{1}{2} \sum_{k=1}^{N_2} U_{a/\mathrm{Hm}} I_\mathrm{m} M_k \int_0^{\tau_k} (\cos(2\omega_0 t + \theta_k + \varphi_k) - \cos(\theta_k - \varphi_k)) dt$$

$$= \sum_{k=1}^{N_2} \frac{U_{a\mathrm{ifm}} I_\mathrm{m} M_k}{4\omega_0} \sin(2\omega_0 t + \theta_k + \varphi_k) \Bigg|_0^{\tau_k}$$

$$- \frac{1}{2} \sum_{k=1}^{N_2} U_{a\,\mathrm{dim}} I_\mathrm{m} M_k \tau_k \cos(\theta_k - \varphi_k)$$

$$= \sum_{k=1}^{N_2} \frac{U_{a\hat{\imath}\mathrm{m}} I_\mathrm{m} M_k}{4\omega_0} \sin(2\omega_0 \tau_k + \theta_k + \varphi_k)$$

$$- \sum_{k=1}^{N_2} \frac{U_{a/\mathrm{im}} I_\mathrm{m} M_k}{4\omega_0} \sin(\theta_k + \varphi_k) - \frac{1}{2} \sum_{k=1}^{N_2} U_{a/\mathrm{im}} I_\mathrm{m} M_k \tau_k \cos(\theta_k - \varphi_k) \tag{34}$$

In Eq. (34), the first two terms are random variables, and the sum of multiple fluctuations will tend to zero. Similar to Eq. (31), the last term must be positive. Therefore, combining Eqs. (33) and (34), the following conclusion can be drawn:

$$W_{IS\_V2G} < 0 \tag{35}$$

3.3 Power Generated by Distortion Voltage and Fundamental Current

Combining Eqs. (17) and (18), the average power generated by the distortion voltage and fundamental current of point a is as follows:

$$
\begin{aligned}
P_{SI\_V2G} &= \sum_{k=1}^{N_2} \frac{1}{T_2} \int_{T_1}^{T_1+T_2} (-R_l I_\mathrm{m} \alpha_k(t) \sin(\omega_0 t + \varphi_k) \cdot (-I_\mathrm{m} \sin(\omega_0 t + \varphi_k))) \, dt \\
&= \frac{1}{2} \sum_{k=1}^{N_2} \frac{1}{T_2} \int_{T_1}^{T_1+T_2} R_l I_\mathrm{m}^2 \alpha_k(t) (1 - \cos(2\omega_0 t + 2\varphi_k)) \, dt \\
&> \frac{1}{2} \sum_{k=1}^{N_2} \frac{1}{T_2} \int_{T_1}^{T_1+T_2} R_l I_\mathrm{m}^2 \alpha_k(t) \, dt - \frac{1}{2} \sum_{k=1}^{N_2} \frac{1}{T_2} \int_{T_1}^{T_1+T_2} R_l I_\mathrm{m}^2 \alpha_k(t) \, dt = 0
\end{aligned}
\tag{36}
$$

Therefore, the following conclusion can be drawn:

$$W_{SI\_V2G} = T_2 P_{SI\_V2G} > 0 \tag{37}$$

3.4 Distortion Power

Combining (17) and (19), the average distortion power at point a is as follows:

$$
\begin{aligned}
P_{S\_V2G} &= \sum_{k=1}^{N_2} \frac{1}{T_2} \int_{T_1}^{T_1+T_2} \left\{ \begin{array}{l} -R_l I_\mathrm{m} \alpha_k(t) \sin(\omega_0 t + \varphi_k) \\ \cdot (-I_\mathrm{m} \alpha_k(t) \sin(\omega_0 t + \varphi_k)) \end{array} \right\} dt \\
&= \frac{1}{2} \sum_{k=1}^{N_2} \frac{1}{T_2} \int_{T_1}^{T_1+T_2} R_l I_\mathrm{m}^2 \alpha_k(t)^2 (1 - \cos(2\omega_0 t + 2\varphi_k)) \, dt \\
&> -\frac{1}{2} \sum_{k=1}^{N_2} \frac{1}{T_2} \int_{T_1}^{T_1+T_2} R_l I_\mathrm{m}^2 \alpha_k(t)^2 \, dt \\
&\quad + \frac{1}{2} \sum_{k=1}^{N_2} \frac{1}{T_2} \int_{T_1}^{T_1+T_2} R_l I_\mathrm{m}^2 \alpha_k(t)^2 \, dt = 0
\end{aligned}
\tag{38}
$$

Therefore, the following conclusion can be drawn:

$$W_{S\_V2G} > 0 \tag{39}$$

Based on the above analysis, the following conclusions can be drawn when the electric vehicle is discharged:

$W_{I\_V2G} < 0$, the fundamental energy is negative. Electric vehicles supply power to the grid, so this part of the electricity should be measured.

$W_{IS\_V2G} < 0$, the energy generated by the fundamental voltage and the distorted current is negative. This part of the electrical energy is also provided by the electric vehicle, so it needs to be measured.

$W_{SI\_V2G} > 0$, the energy generated by the distortion voltage and the fundamental current is positive. The grid side returns electric energy to the electric vehicle in the form of a fundamental current, which should be used to offset the total absorbed energy and should be metered.

$W_{S\_V2G} > 0$, the distortion energy is positive. Although this part of the electric energy is fed back to the electric vehicle by the grid side, it is fed back in the form of distorted current, which is harmful to electric vehicles. This part of the electrical energy should not offset the total absorbed energy and should not be measured.

Energy analysis when electric vehicle charging is similar to that of discharging, and can be directly obtained by combining literature [34]. Therefore, this article will not be deduced in detail.

According to Table 1, the total electrical energy at the metering point is as follows:

Table 1: Results of electric energy analysis

	W_I	W_{IS}	W_{SI}	W_S
Charge (G2V)	>0	>0	<0	<0
Discharge (V2G)	<0	<0	>0	>0
Is it measured?	yes	yes	yes	no

$$W = W_{G2V} + W_{V2G}$$
$$= W_{I\_G2V} + W_{IS\_G2V} + W_{SI\_G2V} + W_{I\_V2G} + W_{IS\_V2G} + W_{SI\_V2G} \tag{40}$$

However, current metering devices simply add up four types of electrical energy without taking into account the effects of distorted electrical energy on the grid and electric vehicles. Currently, the energy at metering point a is as follows:

$$W_a = W_{I\_G2V} + W_{IS\_G2V} + W_{SI\_G2V} + W_{S\_G2V}$$
$$+ W_{I\_V2G} + W_{IS\_V2G} + W_{SI\_V2G} + W_{S\_V2G} \tag{41}$$

Combined with Eqs. (40) and (41), a reasonable measurement formula can be described as follows:

$$W = W_a - W_{S\_G2V} - W_{S\_V2G}$$
$$= W_a - W_S \tag{42}$$

4 Simulation and Result Verification

A reasonable measurement method for electric vehicles during charging has been verified in literature [34]. Next, this paper will verify the reasonable measurement method during discharging. The simulation was performed in the MATLAB 2015b environment. Assume the line load $Z_l = R_l = 1\ \Omega$. Grid voltage is standard sinusoidal voltage. $f_0 = 50$ Hz, $U_m = 220$ V as follows:

$$u(t) = 220 \sin(100\pi t) \tag{43}$$

During the measurement time, the number of occurrences of the distortion signal, the time of occurrence, the duration, and the amplitude are random. The amplitude of the impact signal can be several times the amplitude of the current. The duration can be several seconds or even tens of seconds. Assume that the fundamental period is $T_0 = 0.02$ s. Suppose the number of occurrences of an impact signal or the fluctuation signal is $N = 64$. There is $T = NT_0$.

4.1 Simulation Case 1

It is assumed that only the impact signal is included in the distortion current. When an impact signal is present, according to Eqs. (2) and (8), the current at the metering point a can be expressed as follows:

$$i_a(t) = -(1 + \alpha_1(t)) I_m \sin(\omega_0 t + \phi) \tag{44}$$

$$\alpha_1(t) = \begin{cases} 2e^{-200t}, & t \in [t_{01}, t_{01} + 0.005] \\ 0, & \text{other} \end{cases} \tag{45}$$

where t_{01} is the time at which $\alpha_1(t)$ occurs. Let the current amplitude $I_m = 10$ A flowing into the metering point a, and the currents' phase $\phi = -\pi/50$. Therefore, the current expression flowing into the metering point a can be described as follows:

$$i_a(t) = \begin{cases} -10 \sin\left(100\pi t - \frac{\pi}{50}\right) - 20e^{-200t} \sin\left(100\pi t - \frac{\pi}{50}\right), & t \in [t_{01}, t_{01} + 0.005] \\ -10 \sin\left(100\pi t - \frac{\pi}{50}\right), & \text{other} \end{cases} \tag{46}$$

The voltage at point a is as follows:

$$u_a(t) = \begin{cases} \begin{cases} 220\sin(100\pi t) - 10\sin\left(100\pi t - \dfrac{\pi}{50}\right) \\ -20e^{-200t} \sin\left(100\pi t - \dfrac{\pi}{50}\right) \end{cases}, & t \in [t_{01}, t_{01} + 0.005] \\ 220\sin(100\pi t) - 10\sin\left(100\pi t - \dfrac{\pi}{50}\right), & \text{other} \end{cases} \tag{47}$$

Taking several random impact signals as an example, the current and voltage at the metering point a when the electric vehicle is discharged are drawn, as shown in Fig. 2.

As can be seen from Fig. 2, the current distortion caused by impact signals can cause the voltage to drop. The simulation results of the electric vehicle discharge energy under the impact signal condition can be obtained, as shown in Table 2.
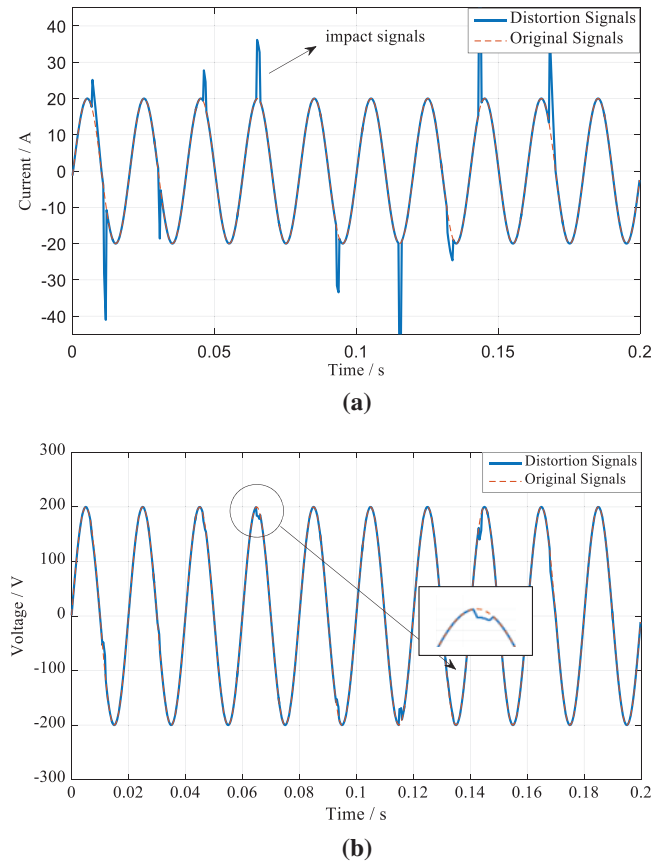
(a)

(b)

Figure 2: Discharge current and voltage under the condition of impact signals. (a) Current flowing into the metering point *a*; (b) Voltage at the metering point *a*

Table 2: Case 1 simulation results under the condition of impact signals

	W_{I_V2G}/J	W_{IS_V2G}/J	W_{SI_V2G}/J	W_{S_V2G}/J
First group	−1341.22	−26.09	1.26	2.10
Second group	−1341.22	−21.78	1.05	1.59
Third group	−1341.22	−25.38	1.22	1.90
Is it measured?	yes	yes	yes	no

As can be seen from the data in Table 2, the simulation results of the four-part electric energy during discharge are consistent with the analysis results in Table 1, that is, $W_{I\_\text{V2G}} < 0$, $W_{IS\_\text{V2G}} < 0$, $W_{SI\_\text{V2G}} > 0$ and $W_{S\_\text{V2G}} > 0$. Therefore, under the impact signal condition, the rationality of the proposed measurement method can be verified.

4.2 Simulation Case 2

It is assumed that only the fluctuating signal is included in the distortion current. When a fluctuating signal is present, according to Eqs. (3) and (8), the current at the metering point *a* can be expressed as follows:

$$i_a(t) = -\left(1 + \alpha_2(t)\right) I_m \sin\left(\omega_0 t + \phi\right) \tag{48}$$

$$\alpha_2(t) = \begin{cases} 0.5, & t \in [t_{02}, t_{02} + 0.06] \\ 0, & \text{other} \end{cases} \tag{49}$$

where t_{02} is the time at which $\alpha_2(t)$ occurs. Let the current amplitude $I_m = 10$ A flowing into the metering point a, and the currents' phase $\phi = -\pi/50$. Therefore, the current expression flowing into the metering point a can be described as follows:

$$i_a(t) = \begin{cases} -15 \sin\left(100\pi t - \frac{\pi}{50}\right), & t \in [t_0, t_0 + 0.06] \\ -10 \sin\left(100\pi t - \frac{\pi}{50}\right), & \text{other} \end{cases} \tag{50}$$
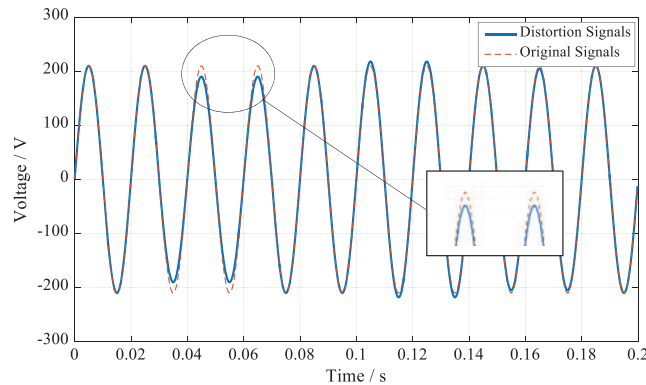
The voltage at point a is as follows:

$$u_a(t) = \begin{cases} 220 \sin\left(100\pi t\right) - 15 \sin\left(100\pi t - \frac{\pi}{50}\right), & t \in [t_0, t_0 + 0.06] \\ 220 \sin\left(100\pi t\right) - 10 \sin\left(100\pi t - \frac{\pi}{50}\right), & \text{other} \end{cases} \tag{51}$$

Taking several random fluctuating signals as an example, the current and voltage at the metering point a when the electric vehicle is discharged are drawn, as shown in Fig. 3.
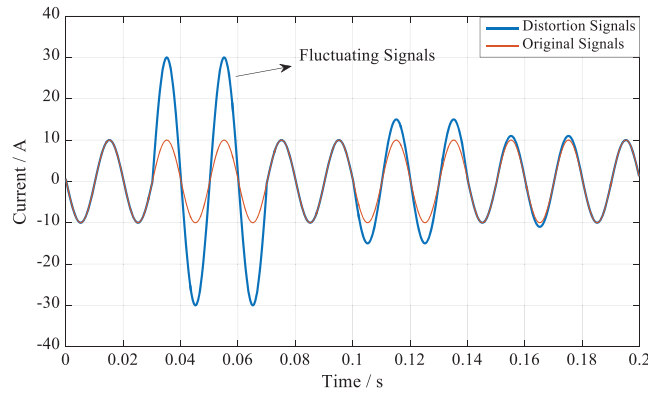
Figure 3: Discharge current and voltage under the condition of fluctuating signals. (a) Current flowing into the metering point a; (b) Voltage at the metering point a

As can be seen from Fig. 3, the fluctuating signals can cause the metering point current to rise and the voltage to drop. Assuming that the number of occurrences of the fluctuating signal is $N = 64$, the simulation results of the electric vehicle discharge energy under the fluctuating signal condition can be obtained, as shown in Table 3.

Table 3: Case 2 simulation results under the condition of fluctuating signals

	W_{I_V2G}/J	W_{IS_V2G}/J	W_{SI_V2G}/J	W_{S_V2G}/J
First group	−1341.22	−54.33	2.87	4.50
Second group	−1341.22	−58.54	2.94	4.77
Third group	−1341.22	−63.72	3.29	5.21
Is it measured?	yes	yes	yes	no

As can be seen from Table 3, under the fluctuating signal condition, there is $W_{I\_V2G} < 0$, $W_{IS\_V2G} < 0$, $W_{SI\_V2G} > 0$ and $W_{S\_V2G} > 0$, which is consistent with the theoretical analysis in Table 1 when electric vehicles discharging.

4.3 Simulation Case 3

Assuming that the distortion signal does not contain the impact signal or the fluctuating signal, the distortion signal degenerates into a harmonic signal. Under the condition of harmonic signals, the current expression flowing into the metering point a can be described as follows:

$$i_a(t) = -10\sin\left(100\pi t - \frac{\pi}{50}\right) - 5.5\sin\left(300\pi t + \frac{\pi}{6}\right)$$
$$-3.5\sin\left(100\pi t + \frac{2\pi}{5}\right) - 2.5\sin\left(700\pi t + \frac{\pi}{4}\right) \tag{52}$$

The voltage at point a is as follows:

$$u_a(t) = 220\sin(100\pi t) - 10\sin\left(100\pi t - \frac{\pi}{50}\right)$$

$$-5.5\sin\left(300\pi t + \frac{\pi}{6}\right) - 3.5\sin\left(100\pi t + \frac{2\pi}{5}\right)$$

$$-2.5\sin\left(700\pi t + \frac{\pi}{4}\right) \tag{53}$$

According to the above, the current and voltage at the metering point a when the electric vehicle is discharged can be drawn, as shown in Fig. 4. And the simulation results are shown in Table 4.

As can be seen from Table 4, under the harmonic signal condition, there is $W_{I\_V2G} < 0$, $W_{IS\_V2G} = 0$, $W_{SI\_V2G} = 0$ and $W_{S\_V2G} > 0$. Therefore, the proposed energy metering method is applicable not only to impact signals and fluctuating signals, but also to harmonic signals.
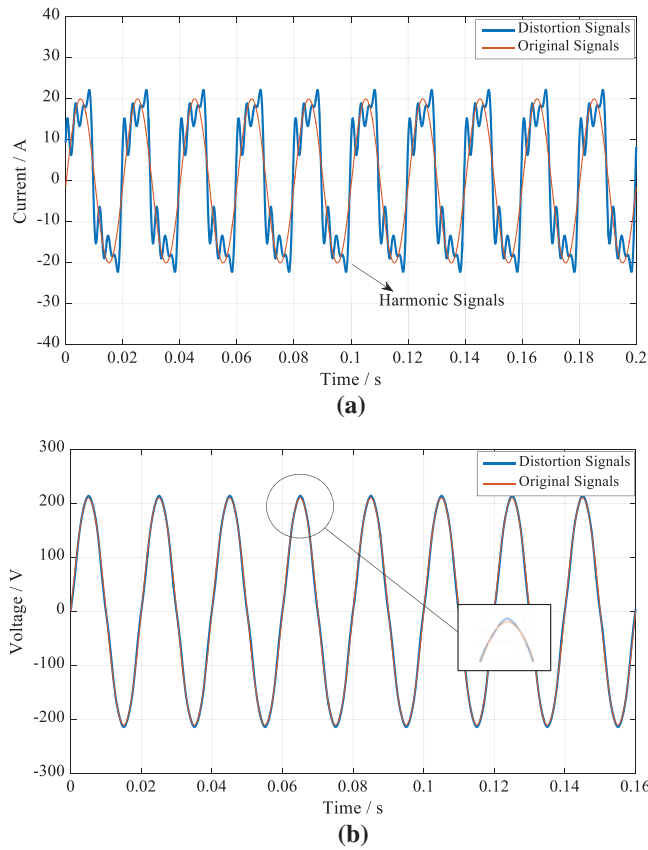
Figure 4: Discharge current and voltage under the condition of harmonic signals. (a) Current flowing into the metering point *a*; (b) Voltage at the metering point *a*

Table 4: Case 3 simulation results under the condition of harmonic signals

	W_{I_V2G}/J	W_{IS_V2G}/J	W_{SI_V2G}/J	W_{S_V2G}/J
First group	-1341.22	0	0	40.16
Second group	-1341.22	0	0	24.80
Third group	-1341.22	0	0	31.20
Is it measured?	yes	–	–	no

In the V2G system, the reasonable measurement method of electric vehicle discharging energy at the metering point is as follows:

$$W_{V2G} = W_{I\_V2G} + W_{IS\_V2G} + W_{SI\_V2G} \tag{54}$$

The reasonable measurement of electric vehicle charging energy has been verified in literature [34], as follows:

$$W_{G2V} = W_{I\_G2V} + W_{IS\_G2V} + W_{SI\_G2V} \tag{55}$$

When the circuit contains only harmonic signals, there is:

$$W_{IS\_V2G} = W_{SI\_V2G} = W_{IS\_G2V} = W_{SI\_G2V} = 0 \tag{56}$$

In summary, a reasonable method of measuring electric energy is as follows:

$$
\begin{aligned}
W &= W_{I\_G2V} + W_{IS\_G2V} + W_{SI\_G2V} + W_{I\_V_{2G}} + W_{IS\_V_{2G}} + W_{SI\_V2G} \\
&= W_a - W_{S\_G2V} - W_{S\_V2G} \\
&= W_a - W_S \tag{57}
\end{aligned}
$$

where W_a is the electric energy metered by the electric energy meter, and W_S is the total distorted electric energy.

5 Conclusions

First, the article points out that the traditional energy metering method in the grid under the distortion signal cannot measure correctly for V2G. Secondly, this paper establishes a load model for the bidirectional interaction of electric vehicles that can be used for energy metering. The power at the measuring point is analyzed, and a reasonable electric energy metering formula is summarized. The V2G bidirectional interaction model can express the charging and discharging process of the electric vehicle more practical and calculate the electric energy more reasonably at the metering point in a certain period.

Although a reasonable metering method is given, meeting the electric energies more accurately based on the V2G bidirectional interaction model is an important issue for engineering applications. The following issues are our future work:

(1) Accurate metering methods based on modern signal processing theories, such as wavelet, time-frequency analysis, and so on.
(2) Metering instruments development with real-time demands based on embedded technologies.
(3) The bidirectional control scheme of EVs for V2G and G2V applications.

Conflicts of Interest: The authors declare that they have no conflicts of interest to report regarding the present study.

References

1. IEA (2020). Energy efficient buildings in Armenia: A roadmap. https://www.iea.org/reports/energy-efficient-buildings-in-armenia-a-roadmap.
2. IEA (2019). Global electric car stock, 2010–2019. https://www.iea.org/data-and-statistics/charts/global-electric-car-stock-2010-2019.
3. Habib, S., Kamran, M., Rashid, U. (2015). Impact analysis of vehicle-to-grid technology and charging strategies of electric vehicles on distribution networks–A review. *Journal of Power Sources, 277(4),* 205–214. DOI 10.1016/j.jpowsour.2014.12.020.

4. Amin, A., Tareen, W. U. K., Usman, M. (2020). A Review of optimal charging strategy for electric vehicles under dynamic pricing schemes in the distribution charging network. *Sustainability, 12(23),* 10160. DOI 10.3390/su122310160.

5. Ota, Y., Taniguchi, H., Nakajima, T., Liyanage, K. M., Baba, J. et al. (2012). Autonomous distributed V2G (Vehicle-to-Grid) satisfying scheduled charging. *IEEE Transactions on Smart Grid, 3(1),* 559–564. DOI 10.1109/TSG.2011.2167993.

6. Liu, P., Wang, C. Y., Hu, J., Fu, T. T., Cheng, N. et al. (2020). Joint route selection and charging discharging scheduling of EVs in V2G energy network. *IEEE Transactions on Vehicular Technology, 69(10),* 10630–10641. DOI 10.1109/TVT.2020.3018114.

7. Madawala, U. K., Thrimawithana, D. J. (2011). A bidirectional inductive power interface for electric vehicles in V2G systems. *IEEE Transactions on Industrial Electronics, 58(10),* 4789–4796. DOI 10.1109/TIE.2011.2114312.

8. Das, D., Weise, N., Basu, K., Baranwal, R., Mohan, N. (2019). A bidirectional soft-switched DAB-based single-stage three-phase AC-DC converter for V2G application. *IEEE Transactions on Transportation Electrification, 5(1),* 186–199. DOI 10.1109/TTE.2018.2886455.

9. Quilez, M. G., Abdel–Monem, M., El Baghdadi, M., Yang, Y., van Mierlo, J. (2018). Modelling, analysis and performance evaluation of power conversion unit in G2V/V2G application–A review. *Energies, 11(5),* 1082. DOI 10.3390/en11051082.

10. Khan, S. U., Mehmood, K. K., Haider, Z. M., Bukhari, S. B. A., Lee, S. J. et al. (2018). Energy management scheme for an EV smart charger V2G/G2V application with an EV power allocation technique and voltage regulation. *Applied Sciences-Basel, 8(4),* 648. DOI 10.3390/app8040648.

11. Battistelli, C., Baringo, L., Conejo, A. J. (2012). Optimal energy management of small electric energy systems including V2G facilities and renewable energy sources. *Electric Power Systems Research, 92,* 50–59. DOI 10.1016/j.epsr.2012.06.002.

12. Ebrahimi, M., Rastegar, M., Mohammadi, M., Palomino, A., Parvania, M. (2020). Stochastic charging optimization of V2G-capable PEVs, A comprehensive model for battery aging and customer service quality. *IEEE Transactions on Transportation Electrification, 6(3),* 1026–1034. DOI 10.1109/TTE.2020.3005875.

13. Richardson, D. B. (2013). Electric vehicles and the electric grid, A review of modeling approaches, impacts, and renewable energy integration. *Renewable & Sustainable Energy Reviews, 19(1),* 247–254. DOI 10.1016/j.rser.2012.11.042.

14. Hannan, M. A., Hoque, M. M., Mohamed, A., Ayob, A. (2017). Review of energy storage systems for electric vehicle applications, issues and challenges. *Renewable & Sustainable Energy Reviews, 69(7),* 771–789. DOI 10.1016/j.rser.2016.11.171.

15. Krueger, H., Cruden, A. (2018). Modular strategy for aggregator control and data exchange in large scale Vehicle-to-Grid (V2G) applications. *Energy Procedia, 151(2),* 7–11. DOI 10.1016/j.egypro.2018.09.019.

16. Hu, X., Wang, K., Liu, X., Sun, Y., Li, P. et al. (2018). Energy management for EV charging in software-defined green vehicle-to-grid network. *IEEE Communications Magazine, 56(5),* 156–163. DOI 10.1109/MCOM.2018.1700858.

17. He, D., Chan, S., Guizani, M. (2018). Privacy-friendly and efficient secure communication framework for V2G networks. *IET Communications, 12(3),* 304–309. DOI 10.1049/iet-com.2017.0608.

18. Shen, G., Su, Y., Zhang, M. (2018). Secure and membership-based data sharing scheme in V2G networks. *IEEE Access, 6,* 58450–58460. DOI 10.1109/ACCESS.2018.2874622.

19. Li, G., Wu, J., Li, J., Ye, T., Morello, R. (2017). Battery status sensing software-defined multicast for V2G regulation in smart grid. *IEEE Sensors Journal, 17(23),* 7838–7848. DOI 10.1109/JSEN.2017.2731971.

20. Wang, S., Wu, J., Zhang, S., Wang, K. (2018). SSDS, a smart software-defined security mechanism for vehicle-to-grid using transfer learning. *IEEE Access, 6,* 63967–63975. DOI 10.1109/ACCESS.2018.2870955.

21. Chen, K., Niu, Y. (2019). Real-time scheduling strategy of electric vehicle based on vehicle-to-grid application. *Power System Protection and Control, 47(14),* 1–9.

22. Zhang, Y., Liu, Q., Hong, C., Tang, G. (2019). Charging and discharging dispatch strategy of regional V2G based on fuzzy control. *Electric Power Automation Equipment, 39(7),* 147–153. DOI 10.16081/j.issn.1006-6047.2019.07.022.

23. Chen, Z., Wang, C., Chen, J., Cai, J., Xue, H. (2019). Study on coordinated charging and discharging control model of electric vehicles under V2G mode. *Zhejiang Electric Power, 38(8),* 37–42.

24. Ge, Z. Q. (2017). Review on data-driven modeling and monitoring for plant-wide industrial processes. *Chemometrics and Intellgent Laboratory Systems, 171(12),* 16–25. DOI 10.1016/j.chemolab.2017.09.021.

25. Yang, X., Zhang, Y., Shardt, Y., Li, X. L., Cui, J. R. et al. (2020). A KPI-based soft sensor development approach incorporating infrequent, variable time delayed measurements. *IEEE Transactions on Control Systems Technology, 28(6),* 2523–2531. DOI 10.1109/TCST.2019.2929478.

26. Zhu, J. L., Ge, Z. Q., Song, Z. H. (2018). Review and big data perspectives on robust data mining approaches for industrial process modeling with outliers and missing data. *Annual Reviews in Control, 46(12),* 107–133. DOI 10.1016/j.arcontrol.2018.09.003.

27. Zhao, S. Y., Huang, B., Liu, F. (2017). Linear optimal unbiased filter for time-variant systems without apriori information on initial conditions. *IEEE Transactions on Automatic Control, 62(2),* 882–887. DOI 10.1109/TAC.2016.2557999.

28. Zhao, S. Y., Huang, B. (2020). Trial-and-error or avoiding a guess? Initialization of the Kalman filter. *Automatica, 121(21),* 109184. DOI 10.1016/j.automatica.2020.109184.

29. Hanani, U., Shapira, B., Shoval, P. (2001). Information filtering, overview of issues, research and systems. *User Modeling and User-Adapted Interaction, 11(3),* 203–259. DOI 10.1023/A:1011196000674.

30. Zhao, S. Y., Yuriy, S., Shmaliy, A. C., Zhao, C. H. (2020). Probabilistic monitoring of correlated sensors for nonlinear processes in state space. *IEEE Transactions on Industrial Electronics, 67(3),* 2294–2303. DOI 10.1109/TIE.2019.2907505.

31. Yang, X., Gao, J. J., Huang, B. (2021). Data-driven design of fault detection and isolation method for distributed homogeneous systems. *Journal of the Franklin Institute, 358(9),* 4929–4949. DOI 10.1016/j.jfranklin.2021.04.016.

32. Huang, J., Yang, X., Peng, K. X. (2021). Double layer distributed monitoring based on sequential correlation information for large-scale industrial processes in dynamic and static states. *IEEE Transactions on Industrial Informatics, 17(9),* 6419–6428. DOI 10.1109/TII.2020.3019499.

33. Zhang, X., Li, Y., Cao, W. (2016). Method of active power measurement under condition of distortion signal. *Journal of Electric Machines and Control, (6),* 87–93. DOI 10.15938/j.emc.2016.06.011.

34. Cui, J., Zhou, J., Xu, Z., Zhang, Z., Li, Q. (2018). *Review of active power measuring methods for vehicle-to-grid (V2G),* pp. 1448–1453. Xi'an, China: CAC.